



UNIVERSITY OF PADOVA

Department of General Psychology*

**Master Degree in Cognitive Neuroscience and Clinical
Neuropsychology**

Final dissertation

**Investigating Gray Matter Network Alterations in Preclinical
Alzheimer's Disease Using Graph Theoretical Measures**

Supervisor

Professor / PhD Aron Emmi (Department of Neuroscience, University of Padua)

Co-supervisor (if present)**

Professor / PhD Raffaele Cacciaglia (Researcher at Barcelona Beta Brain Research Center)

Candidate: Elif Harput

Student ID number: 2071336

Academic Year 2023/2024

Abstract

Alzheimer's Disease (AD) is the leading cause of dementia. Given the growing number of older population, it becomes a concerning healthcare issue. The brain begins to deteriorate several years before the emergence of clinical symptoms. AD is characterized by neuronal and synaptic degeneration, accumulation of amyloid beta plaques and tau tangles. Besides, changes in gray matter networks have been reported in early stages of the disease which have been associated with amyloid beta deposition and tau pathology. In this study, we investigated the relationship between changes in gray matter networks and biomarkers of amyloid beta and tau in preclinical AD cohort by using graph theoretical measures. We included 362 cognitively unimpaired individuals. We examined which graph properties were changed across individuals. On a global level, we found increased average path length, average betweenness centrality, and gamma, lambda and small world values were increased when p-tau levels were higher. Regionally, significant relationship was found between p-tau levels and betweenness centrality in left superior frontal gyrus orbital. Furthermore, average clustering measure had a significant association with lobule 1-2 of vermis. Findings suggest that in the preclinical stage, gray matter properties show changes and this can be used to identify future clinical symptom progression in AD research.

Contents

<i>Introduction & General Overview</i>	5
Alzheimer's Disease Clinical Progression.....	5
Biomarkers & Pathophysiological Continuum of AD	6
Risk Factors for AD	10
Gray Matter Networks	12
Graph Theory and Properties	13
Gray Matter Network Changes in AD	15
Study Aim	20
<i>Materials & Methods</i>	21
Single Subject Gray Matter Network Analysis.....	21
MATLAB Script Explanation	22
Participants.....	23
Statistical Analysis.....	24
<i>Results</i>	25
Subjects.....	25
<u>Global Analysis</u>	26
Relationship between CSF A β 42/A β 40 and CSF p-tau levels and global gray matter network measures in whole group	26
Interaction Models	27
Main effects of sex and age on global gray matter network measures	28
Relationship between CSF A β 42/A β 40 ratio and CSF p-tau levels and global gray matter network measures in different AT groups	29
<u>Regional Analysis</u>	30
Relationship between CSF A β 42/A β 40 ratio and regional gray matter network measures.....	30
Relationship between CSF p-tau levels and regional gray matter network measures	32

Investigating Gray Matter Network Alterations in Preclinical Alzheimer's Disease Using Graph Theoretical Measures	4
<i>Discussion</i>	34
<i>References</i>	38

Introduction & General Overview

What is Alzheimer's Disease

Alzheimer's Disease (AD) is the most common neurodegenerative disease, representing the cause for 60-70% of cases of dementia. Together with cardiovascular diseases, neurodegenerative diseases such as AD represent a concerning socio-economic and healthcare burden, particularly due to the rapid aging of the population.

From a pathological standpoint, AD is characterized by a chronic degenerative process leading to neuronal and synaptic loss, associated to the presence of amyloid beta plaques and tau neurofibrillary tangles. Changes in the brain begin several years before the onset of the first clinical symptoms (Jack et al., 2010). Amyloid beta starts to accumulate 20-30 years before the onset of symptoms, while biomarkers of neurodegeneration start to form just before the onset of symptoms (ten Kate et al., 2018a). Over the past years the definition of AD has been changed considerably due to in vivo evidence of specific biomarkers underlying AD neuropathology. This definition and identification of AD can have major implications for diagnosis and comprehension of the disease progression. While the definitive diagnosis of AD still relies on the postmortem examination in the brain, recent developments in laboratory and neuroimaging biomarkers allow for a more accurate in vivo evaluation (Dubois et al., 2010). According to the criteria of Dubois et al (2010), a diagnosis of AD can be reached when there is both clinical evidence of the disease phenotype and in vivo biological evidence of AD pathology (Dubois et al., 2010). Furthermore, with developing research in the field of neurodegenerative diseases how researchers understand AD is continuously changing.

Alzheimer's Disease Clinical Progression

The progression, staging and different disease phenotypes underlying AD have been described through various models in literature. In their study, Jack and colleagues (2010) defined three disease stages of AD. The first one is the pre-symptomatic stage in which individuals are cognitively unimpaired but have AD pathological changes. Secondly, there is the prodromal AD that is equivalent to mild cognitive impairment (MCI) in which individuals experience the earliest symptoms such as memory problems. MCI is characterized by subtle cognitive decline that is more than expected for an individual's age but not severe enough to interfere with daily life activities. MCI can be considered a precursor to AD, but there are differences in terms of its severity, daily functioning, brain changes and diagnostic criteria in comparison to AD pathology. The last stage is the formation of AD pathology in which

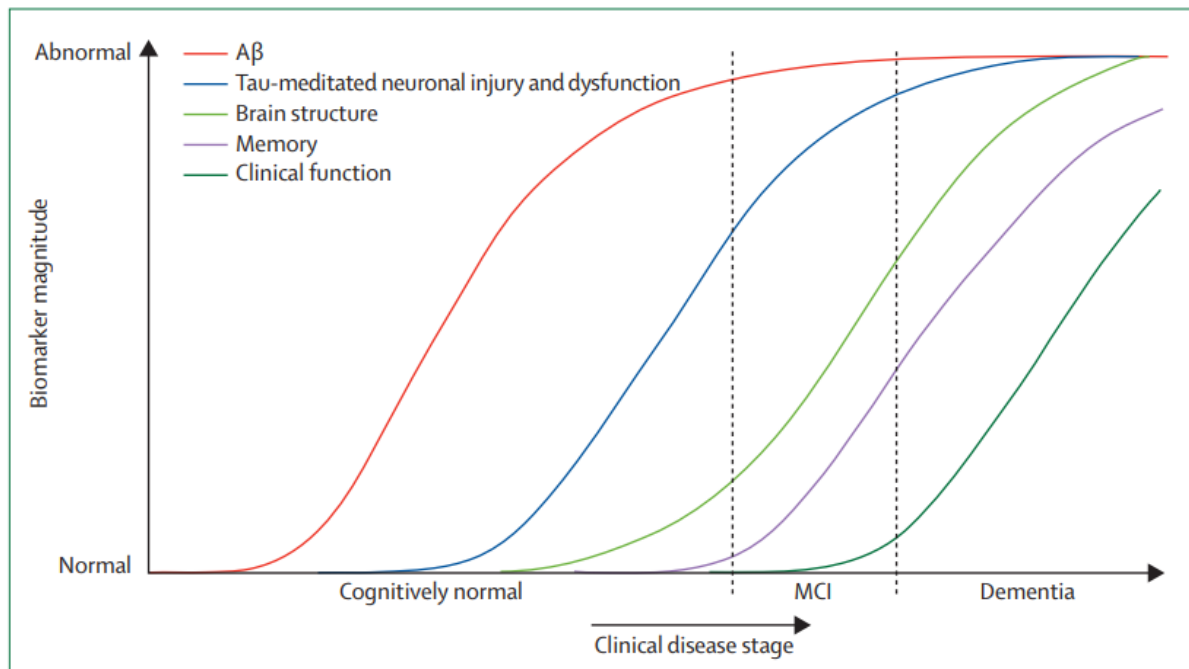
people experience impairments in multiple domains (Jack et al., 2010). In another study by Sperling et al (2011) to disentangle the biological and clinical processes they used AD-pathophysiological (AD-P) changes to refer to underlying brain changes and AD-clinical (AD-C) to refer to the occurrence of clinical and cognitive symptoms. AD-P occurs a long time before AD-C. Individuals who have AD-P biomarker evidence are likely to progress to AD dementia. However, some individuals do not experience any clinical symptoms in their life (Sperling et al., 2011).

The first stage of AD pathology is mostly named as preclinical AD, referred to before as pre-symptomatic AD and AD-P. In this thesis the term preclinical AD will be used. Preclinical AD spans from the first neuropathology in the brain until the onset of the first clinical symptoms of AD. There are two different kinds of preclinical phases of AD. Asymptomatic at-risk individuals have evidence of biomarker A β accumulation but no evidence of tau or neurodegeneration. They are cognitively unimpaired. However, the value of these biomarker changes is absent and not enough to predict further development of the disease. Presymptomatic AD individuals will develop AD pathology due to genetic mutation, but they still do not show any symptoms (Dubois et al., 2010). Overall, the concept of the AD spectrum characterizes the heterogeneity of the disease, encompassing a continuum from preclinical stages marked by subtle neuropathological changes to the emergence of clinical symptoms. Biomarkers and underlying pathophysiological mechanisms serve as crucial tools for understanding these distinct phases along the disease trajectory.

Biomarkers & Pathophysiological Continuum AD

Biomarkers are physiological, biochemical, or anatomical indicators that reflect specific features of disease related changes (Jack et al., 2010). They may provide a diagnostic tool to identify the disease in early stages (van Oostveen and de Lange 2021). Biomarkers of AD can be categorized into three different classes based on the type of pathophysiology. It is called the “A/T/N” system. “A” refers to the A β biomarker, “T” indicates the tau biomarker and lastly “N” corresponds to neurodegeneration and neural injury. Each biomarker is rated as negative or positive according to their corresponding levels (Jack et al., 2010; Jack et al., 2016). These biomarkers occur at different time points along the AD continuum. According to Figure 1, the first biomarker which becomes abnormal is A β without any cognitive or clinical symptoms present. As the clinical disease stage progresses tau starts to progress which is an indicator of neuronal injury and

dysfunction. In individuals with MCI changes in brain structures can be observed with neuroimaging techniques. Towards late stages of MCI, memory dysfunctions are unavoidable, later followed by observable changes in clinical functions in demented individuals (Jack et al., 2010).



(Jack et al., 2010) **Figure 1: Dynamic biomarkers of the Alzheimer's pathological cascade.** A β is measured by CSF A β 42 or A β PET. Tau mediated neuronal injury and dysfunction is identified by CSF tau or FDG PET. Brain structure is calculated with sMRI.

The initial pathological event in AD is A β deposition which occurs outside of the cell. According to the amyloid cascade hypothesis, AD develops due to a disruption in the balance of A β in the brain. Amyloid precursor protein which is a membrane protein involved in synapse formation and signaling, is responsible for the formation of A β plaques. There are proteins called secretases which cut amyloid precursor protein into shorter pieces called amyloid beta peptides. A β peptides can be of different lengths. In a healthy brain, they are either cleared away into the CSF or carried out of the brain into the bloodstream. In case of an overproduction or disruptions in clearance of A β , these peptides aggregate and form A β plaques (Budelier & Bateman, 2020; Hansson 2021; van Oostveen & de Lange, 2021). The main component of these plaques is a protein called A β 42 (1-42). These plaques absorb A β 42 and lower its levels in the CSF (Budelier & Bateman, 2020). As a result, in individuals with AD decreased levels of CSF A β 42 is observed compared to healthy

individuals (Budelier & Bateman, 2020). Another molecule called A β 40 (1-40) is also produced. However, CSF A β 40 levels did not differ between healthy individuals and individuals with AD (Budelier & Bateman, 2020).

In several studies, a ratio of A β 42/A β 40 is observed. This can help accounting for interindividual differences in A β concentration. Decreased CSF A β 42/A β 40 ratio is used to predict A β deposition in AD (Budelier & Bateman, 2020). Moreover, decrease in CSF A β 42 occurs before other A β measures become abnormal (Budelier & Bateman, 2020; ten Kate et al., 2018b). Neuroimaging methods such as PET and MRI are also used to measure A β levels. Opposite to CSF A β 42 levels, A β PET levels are increased in individuals with AD compared to healthy individuals.

PET scans use special molecules called radioligands which give off tiny positively charged particles. These particles encounter negatively charged electrons and create an energy which releases gamma photons. Detectors in the PET scanner detect these gamma rays and create an image. When measuring A β , radioligands detect A β plaques and stick to them. This way after waiting a short period, PET can select these plaques and make them observable. To develop A β tracers, a brain dye is created called thioflavin-T. This dye binds to A β plaques, can pass through the blood brain barrier and allow the evaluation of A β plaques in vivo. In A β imaging, the first tracer used was made with carbon. First carbon-based tracer was Pittsburgh Compound B (PiB), a carbon-based tracer. Later fluorine-based tracers were developed which allow for longer investigation times compared to carbon-based ones (Marquez & Yassa, 2019). Since these tracers' observability times are different, they have different sensitivities in detecting A β levels (ten Kate et al., 2018b).

Previous research detected the parietal cortex regions, medial temporal lobes and frontal cortex as the earliest regions to get affected by A β plaque deposition. Later when the disease progresses it spreads to other regions in the cortex (Hansson 2021). Progression and changes also depend on structural and functional connectivity between the regions (Marquez & Yassa, 2019). These changes can be observed with structural magnetic resonance imaging (sMRI) and functional MRI (fMRI). In sMRI A β accumulation is initially seen in structures of the default mode network (DMN) such as the medial frontal cortex and medial parietal cortex (Yu et al., 2021). Gray matter atrophy caused by A β deposition can be also detected in sMRI (Ewers et al., 2011). Gray matter is important for information transportation between regions in the cortex. Therefore, in some studies, A β positivity in cognitively healthy patients has been associated with an increased risk of cognitive decline and later continuing in the trajectory of AD (ten Kate et al., 2018b). However, other studies suggested

that since changes in $A\beta$ occurs before any cognitive symptom onset, the relationship between $A\beta$ burden and changes in cognition is not clearly understood (Marquez & Yassa, 2019). Therefore, other biomarkers such as biomarkers of neurodegeneration or neural injury should be investigated as well.

In healthy individuals, tau is released by neurons and travels through CSF and blood where it is broken down and cleared out. However, the level of tau is relatively low, and it is not phosphorylated. Phosphorylation is a modification of proteins where a phosphate group is attached. When there is abnormal phosphorylation, tau tangles are formed by aggregation. These tangles lead to disruption of communication between neurons. In healthy ageing adults who are over 60 years, tau tangles which are formed by tau protein can be observed mostly in the medial temporal lobe (Hansson, 2021). However, in AD pathology tau tangles spread from the medial temporal lobe and progress towards the neocortex. Most tests assess p-tau 181 (phosphorylated threonine 181), other measures of p-tau are also developed such as p-tau 231 (phosphorylated threonine 231) and p-tau 199 (phosphorylated serine 199). In detecting AD, levels of these p-tau tests can vary significantly (Budelier & Bateman, 2020).

In both healthy individuals and individuals with AD, t-tau or total tau exists which mainly relates to shortened tau fragments (truncated tau). T-tau is produced and released by healthy cells in an opposite manner to full length tau released with neuronal cell death. Although increased levels of p-tau are more specific to AD, changes in levels of t-tau can be due to other neurodegenerative diseases. Increased t-tau levels are related to worse cognitive functions (Budelier & Bateman, 2020). Another way to measure tau is by looking at CSF. Increased CSF tau is not only applicable to AD but to other neurological disorders since it correlates with greater cognitive impairment and disease severity. In AD, increased CSF tau may occur as a direct consequence of tau accumulation in axons (Jack et al., 2010). Neuroimaging such as PET scan can also be used to investigate tau levels in the brain. Tau first starts to deposit in the medial temporal lobe where the memory system is located, it then spreads from the entorhinal cortex to the hippocampus and then to the rest of the cortex (Yu et al., 2021). Fluorodeoxyglucose PET (FDG PET) measures resting state cerebral metabolic rates of glucose as a signature for neuronal activity, it measures the level of glucose which is associated with cerebral metabolism and synaptic activity. Metabolic abnormalities have been seen in individuals with MCI and AD. (Sperling et al., 2011). These abnormalities occur first in the temporal and parietal lobes and sometimes in the frontal lobe, whereas areas such as sensory and visual areas and the cerebellum are spared.

Beyond being useful in vivo, but biomarkers can also be used post-mortem to evaluate disease stages and phenotypes. Even in individuals who appear cognitively unimpaired, post-mortem examinations often reveal pathological changes indicative of AD. Key post-mortem findings include A β plaques, neurofibrillary tangles, neuronal loss, and brain atrophy. A β plaque distribution is classified using the Thal plaque phase stages, delineate the spread of A β plaques in different brain regions. Neurofibrillary tangle distribution is determined according to the Braak model, which also describes the progression of tangles in various brain areas. There are also neuritic plaques which are primarily composed of A β , formed when A β clumps together and accumulates in the spaces between neurons. The CERAD neuropathology protocol is used to investigate neuritic plaques. By combining these three criteria, the staging and likelihood of AD can be estimated (Love et al., 2014, p.886-888). It is also important to note that while post-mortem staging provides valuable information into discovering new markers and assess outcomes of rapidly emerging treatment strategies, it does not capture the full spectrum of clinical symptoms.

Several previous research proposed that changes in cognitive function in AD are due to disruptions in the structural and functional network connectivity between the regions in the brain (Voevodskaya et al., 2017). There are different types of connectivity, and they can be represented as a connectivity matrix. This matrix consists of nodes which are brain regions in a structural or functional connectome and links which represent the connectivity between two nodes in a structural or functional connectivity (Yu et al., 2021). While talking about network connectivity, it is also important to mention the importance of the gray matter which is crucial for information processing in the brain and can explain connectivity disruptions in AD. Therefore, focusing on gray matter networks can offer a more detailed understanding of how cognitive decline in AD arises.

Risk Factors for AD

In previous research for a long time the common opinion was that women who carry the copy of the $\epsilon 4$ allele of the APOE gene are more prone to develop AD compared to men who also carry the same allele and the same amount. There are 3 different alleles of the APOE gene which are $\epsilon 2$, $\epsilon 3$, and $\epsilon 4$. Only carrying allele $\epsilon 4$ is indicated as a risk factor for developing AD. Contrary, $\epsilon 2$ has a protective effect for AD.

Presence of APOE $\epsilon 4$ may have effects on connections in the brain, and on gray matter organization. In one previous study, Regy and colleagues (2022) investigated the

relationship between APOE $\epsilon 4$ status and regional gray matter in cross sectional and longitudinal analysis using data from a large MEMENTO cohort of individuals with subjective memory complaints without dementia diagnosis. Regy et al (2022) hypothesized that individuals who are APOE $\epsilon 4$ carriers would have smaller gray matter volumes and also have more atrophy rates in regions associated with early neuropathological changes. They found that non-demented APOE $\epsilon 4$ carriers were associated with lower gray matter volume and higher atrophy when they had the follow up session two years later. Regions like the hippocampus and entorhinal cortex were the most vulnerable areas (Regy et al., 2022). These are the areas also first affected by A β deposition and tau pathology.

There have also been some contrary results with findings on the relationship between APOE gene and sex specific effects. To investigate this relationship more, many individual data were used from 27 independent research studies. Neu et al (2017) examined individuals between 55 and 85 years. In this age span the chances of men and women with APOE $\epsilon 3/\epsilon 4$ phenotype on developing AD were equal. However for women, the risk of developing AD increased at younger ages (Neu et al., 2017). Moreover, a comparison was made between transition from cognitively normal to MCI and MCI to AD. APOE $\epsilon 4$ increased the risk to convert from MCI to AD between the ages of 70 to 85 but not between ages of 55 to 69 years (Neu et al., 2017; Regy et al., 2022). It can be the case that the effect of APOE $\epsilon 4$ increases with age, and it does not have a significant influence in relatively younger ages. APOE $\epsilon 4$ alleles' effect is also dependent on changes in biomarkers such as A β and tau. Most of the time, increased levels in these biomarkers (only exception for CSF A β , with age CSF A β decreases) occur with age, so this can change or enhance the influence of APOE $\epsilon 4$ on the development of MCI and AD. These influences can also depend on the cohort, the sample size, and demographics.

Sex-based differences have important effects on and implications for AD regarding future therapeutic approaches or for diagnosis. In normal aging looking at global brain volume men have more reductions due to aging than women. However, only looking at specific regions in the brain such as the hippocampus and parietal lobe, in this case women showed significantly stronger reductions in brain volume compared to men. In AD, previous research found significantly larger frontal impairments in women compared to men (Skup et al., 2011). Women who were between 55 and 70 years had an expanded risk for developing MCI and when they were observed between 65 and 75 their risk to develop AD was increased. These sex specific differences can be associated with changes that occur physiologically with menopause and changes in estrogen levels (Neu et al., 2017). Other

factors to consider when examining the relationship between sex differences and AD include the higher risk of male subjects of experiencing cardiovascular diseases and a stroke compared to women. Longer-lived males may suffer less from other medical conditions, and present comorbid conditions compared to women of the same age, hence the lower risk of developing AD (Neu et al., 2017). To investigate sex differences in specific regions in gray matter, Skup et al (2011) examined cognitively healthy, MCI and AD individuals who are between 55 and 90 years of age from the ADNI cohort in a longitudinal study design. They found that women with MCI and AD had reductions in the right caudate nucleus compared to cognitively healthy women, but they did not observe this effect for men. Sex specific differences were seen in areas such as left insula, thalamus, right middle temporal gyrus. Volume reductions were seen in these areas only for women with AD but not for men. Both men and women with aMCI showed different shrinkage patterns in the thalamus, precuneus, and amygdala compared to men and women with probable AD. Overall, the findings suggest that sex may influence the way gray matter atrophy progresses in MCI and AD.

Gray Matter Networks

Individuals that are healthy and have unimpaired cognitive functioning have efficient communication between neurons. In case of any disruptions in brain networks this communication breaks down and leads to neurological disorders. Due to $A\beta$ accumulation in AD, connections can be disrupted and have an influence on gray matter networks (Dicks et al., 2018, ten Kate et al., 2018a; Yu et al., 2021). These networks are useful and sensitive to capture early brain changes and future cognitive decline. They can be constructed through neuroimaging techniques such as sMRI, fMRI, DTI, and others. Previous research has found, cognitively unimpaired older adults with lower level of CSF $A\beta_{42}$ showed disrupted gray matter network measures in the very early disease stage. Gray matter networks start to get abnormal and disorganized even from the very early stages of the disease (Dicks et al., 2018).

In the preclinical stage, $A\beta$ deposition is related to abnormal regulation of large-scale networks, especially the DMN which is a functional resting state network (Ewers et al., 2011). Some fMRI studies suggested cognitively unimpaired individuals who have increased $A\beta$ in the brain measured by PET and decreased levels of CSF $A\beta_{42}$ in the brain are associated with decreased functional connectivity in regions of DMN (Voevodskaya et al., 2017). Hedden et al (2009) evaluated cognitively unimpaired older adults, investigating whether $A\beta$ is associated to abnormalities in cortical network integrity by using fMRI and

PiB (Pittsburgh Compound B) PET, focusing on the DMN. A comparison between individuals with low (PiB-) and high (PiB+) A β burden was made. Functional connectivity within regions of the DMN was significantly reduced in the PiB+ group. Results suggested that decreased functional connectivity due to high A β burden in DMN is associated with atrophy of hippocampal formation and cortical thinning in DMN regions (Hedden et al., 2009).




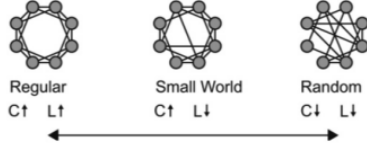
Focusing on gray matter networks offers a deeper understanding of connectivity dysfunctions in AD. By mapping the connections between main processing centers through gray matter networks, a better view is gained on how these disruptions manifest. Analyzing the properties of these networks with graph theory can reveal more information on AD network disruptions.

Graph Theory and Properties

Individuals with AD and individuals who are at risk of developing AD have different structural network organization compared to healthy and not at-risk individuals (Voevodskaya et al., 2017). A very common approach to analyze and observe structural networks is called the graph theoretical approach. This framework allows researchers to examine brain connectivity and network organization. It models the brain as nodes and edges. Nodes represent the anatomical regions and edges indicate connectivity between these regions (Voevodskaya et al., 2017). Graph properties have a big impact on tracking disease severity which can be important for new therapeutic approaches (Tijms et al., 2013a&b). With computation of graph theory matrices, for each of the networks a measurement can be generated indicating the nature of local brain activity such as hubs. Hubs are crucial for information processing, and they increase a network's strength towards a random failure. Graph theory is also beneficial for understanding graphs that have different types of connectivity data. It helps researchers to understand the pathophysiological overview of AD by examining structural and functional disruptions and the disease progression (Tijms et al., 2013b) There are many properties that could be used to describe network structures. Network size is the total number of nodes in the network. Average degree represents average number of connections (edges) per node. Connectivity density is the ratio of all existing connections to the number of connections that are possible in the network. Average clustering coefficient is the proportion of connected nodes that are also interconnected. Average path length indicates the shortest path length between any pair of nodes in the network. Average betweenness centrality assesses which nodes are more centrally connected relative to other

nodes in the network. These nodes will be hubs which have a more central role in the network. Existence of hubs decreases path length and declares graphs more resilient towards random attack of nodes or edges. They are the weakest points of networks that are targeted by neurodegenerative diseases. Networks also can have small world properties which are defined by the small world coefficient. One can get the value by normalizing the average clustering coefficient (γ) and normalizing the path length (λ) of each graph. Normalized means the ratio of the property of the brain network to that of matched random networks. Small world networks are based on segregation and integration. Segregation measure, which is the clustering coefficient, is helpful to understand how information is processed within richly interconnected groups of regions of different functions. Integration measures can be considered in two points of view. Firstly, efficiency of global information communication which is based on characteristic path length. Secondly, the ability of the network to integrate distributed information which is based on network hubs (Dai & He 2014). A network will have a small world property when σ (γ / λ) is bigger than one, suggesting that its topology is different than that of a random graph (Dicks et al., 2020; Pelkmans et al., 2021a; Tijms et al., 2013b). In random networks, connections between nodes are randomly organized (Dai & He, 2014). There are also regular networks, they are very organized and predictable. They have the same number of connections for each node. Information flow is relatively slow in the network. Small world network nodes are well connected with near neighbor nodes but also have shortcut connections. It has a shorter characteristic path length compared to a regular network. Compared to a random network it has greater clustering coefficient. Investigating small world property is crucial because preclinical AD and individuals with AD dementia have more random network organization and this is related to future cognitive decline and impairment (Dicks et al., 2020). In Table 1, the network properties are shown that are used in this thesis for analyzing gray matter network structures. Single subject networks are analyzed both at global brain level and in a region specific localized manner.

Table 1
Overview of studied network properties

Network measure	Global, local	Explanation	Example
(1) Network size	Global	Total number of nodes (i.e., brain areas).	
(2) Connectivity density	Global	Percentage observed connections from the maximum number possible connections.	
(3) Degree	Global, local	The number of connections per node.	
(4) Clustering coefficient	Global, local	Proportion of existing connections between neighboring nodes from the maximum number of possible connections. This is a measure of information segregation, that is, specialized information processing.	The clustering coefficient of the white node would be 0.33, as 1 connection of the 3 possible exists. 
(5) Path length	Global, local	Minimum number of connections to go from one node to another node. This is a measure of information integration, as through, for example, long-range connections distant clusters can exchange information.	The path length between the white and the black node would be 3. 
(6) Betweenness centrality	Global, local	The number of shortest paths that run through a node. This is a centrality measure.	The white node would have the highest betweenness centrality as all short paths run through this node. The network falls apart when this node is removed. 
(7) γ normalized clustering coefficient	Global	Quantifies how the global clustering coefficient of an observed network deviates from that of a random network.	
(8) λ normalized path length	Global	Quantifies how the global path length of an observed network deviates from that of a random network.	
(9) Small-world property	Global	An observed network with $\gamma > 1$ and $\lambda \approx 1$ is "small world," that is, a network balances specialized information processing through clustering and information integration through long-range connections. In a random network path length (L) is minimized, at the expense of a loss of clustering (C). In contrast, a completely regularly organized network has high clustering, at the expense of the highest path length value.	 <p>Regular C↑ L↑ Small World C↑ L↓ Random C↓ L↓</p> <p>← Information segregation Information integration →</p>

(Tijms et al., 2018) *Figure 2: Overview of network properties*

Gray Matter Network Changes in AD

Individuals who are cognitively unimpaired have small world network organizations that provide the most efficient way of information processing compared to individuals with cognitive impairments. This network organization can be disrupted in individuals with AD pathology (Tijms et al., 2013a&b; Tijms et al., 2016; Tijms et al., 2018; Dicks et al., 2018; ten Kate et al., 2018a; Yu et al., 2021) . Gray matter network measures in subjects with MCI who later developed AD were very similar to the organization of gray matter networks in AD participants compared to healthy controls (Tijms et al., 2018). One study by Voevodskaya et al (2017), on group level structural networks, analyzed the changes in structural brain networks and how they may interfere with symptom onset of AD pathology. They used CSF A β 42/A β 40 levels for A β pathology to see if it has any effect on structural connectivity measures in local and global levels. Participants who were cognitively healthy individuals and were older than 60 years with CSF analysis and MRI scan were selected from the BioFINDER cohort. Two groups were created which are individuals who are

healthy controls with normal CSF A β levels and individuals that are cognitively healthy but have abnormal CSF A β levels. To investigate structural networks, graph analysis was applied by examining parameters such as global efficiency, clustering coefficient, transitivity, modularity, and existence of hubs. Global efficiency reflects how efficient the network is, how quickly information can travel between different brain regions. Clustering, transitivity, and modularity represents how regions are organized into specific groups. Hubs are important communication points in a network that are highly connected to many other regions and play an important role in information flow throughout the brain. Individuals with abnormally A β levels had decreased global efficiency, reduced modularity compared to control individuals. Moreover, individuals with elevated levels of A β had disruptions in network hubs. This is an anticipated result since well connected brain regions such as hubs are the most targeted regions by neurodegeneration (Voevodskaya et al., 2017).

It has been found that in cognitively unimpaired older adults, disruptions of gray matter networks have been related to more abnormal A β 42 levels in CSF, indicating that gray matter measures are sensitive to changes from early on in disease continuum (Tijms et al., 2018). It is also known that these networks are more randomly organized in individuals with AD and can lead to faster cognitive and clinical decline. Tijms and colleagues (2018) explored gray matter network disruptions in the AD continuum and if these network disruptions are associated with clinical symptoms. 62 subjects with subjective cognitive decline and 160 subjects with MCI were selected from the Amsterdam Dementia Cohort. They all had abnormal A β 42 CSF levels. A follow up visit was scheduled a year later for every participant. They received a clinical diagnosis of MCI or AD according to a commonly used criterion. Individual gray matter networks were generated, CSF samples were collected and to assess cognitive decline, they performed the Mini Mental State Examination (MMSE). To analyze the network disruptions several graph properties were calculated. After around 2 years some patients showed to have MCI, AD dementia and others developed other types of dementia. During this time some subjects did not show any progression, and some showed an increase in disease continuum. Individuals who progressed to a more severe condition had lower normalized path length and small world values in the global analysis. According to the local analysis done with 90 regions of the automated anatomical labeling (AAL) atlas, patients who progressed had lower clustering values that are mostly in temporal and frontal lobes. The largest change in graph properties was seen in DMN which is an area vulnerable for AD due to being one of the hub regions in the brain. Moreover, individuals who had decreases in graph property measures had lower

scores in MMSE, which means a more disorganized and random gray matter network organization contributed to a cognitive decline. Gray matter network parameters can be useful to identify how fast individuals will progress to AD dementia and regional analysis can be beneficial to see which areas are more vulnerable to these changes (Tijms et al., 2018).

Another previous study by Tijms et al (2016) investigated whether A β 42 CSF levels are associated with changes in single subjects gray matter networks in cognitively unimpaired individuals. 408 individuals' data were analyzed from a longitudinal study on preclinical AD from the Gipuzkoa Alzheimer Project (GAP) who were aged between 39 and 80 years. In order to analyze network structure, network properties were calculated for each subject. They did not find any effect of APOE status as a mediating factor on A β 42 levels and network properties. Decreased A β 42 levels were associated with lower connectivity density values. They further looked into the relationship between A β 42 and network measures distributed across specific regions in the cortex. Lower A β 42 levels were found to be associated with lower clustering values in different areas such as frontal and medial posterior cortex. Overall, the findings suggested that cognitively healthy adults with A β 42 levels within the usual range, exhibit lower connectivity density, longer path length, and weaker clustering in networks. This might be in the very early stages of network disorganization, potentially preceding future cognitive decline (Tijms et al., 2016).

In another study by Tijms and colleagues (2013a), they hypothesized that individuals with AD would exhibit a more random network organization compared to cognitively unimpaired individuals. The study recruited individuals with probable AD and a control group with subjective memory complaints, with a mean age of 72. Network properties such as size, connectivity density, degree, path length, clustering coefficient, betweenness centrality, and small world coefficient were computed. Results showed that path length, clustering coefficient and small world coefficient were decreased at the global level. Specifically, the clustering coefficient and path length showed a decline in the left parahippocampal gyrus, left lingual gyrus, and bilateral thalami in AD patients. Some regions of the DMN also showed local graph disruptions in AD patients. Moreover, they observed the relationship between cognitive decline severity and network alterations. General cognitive decline was measured with MMSE. Path length was highly associated with MMSE scores. Random graph organization was associated with worse cognitive dysfunction in the AD group (Tijms et al., 2013a).

Furthermore, previous research measured A β deposition using PET and investigated disruptions in gray matter networks in cognitively normal older adults with subjective memory complaints. The relationship between A β deposition and gray matter networks was examined. Moreover, the effect of APOE ϵ 4 gene was observed if it is a mediator between A β accumulation and gray matter network changes. Researchers used a population from the INSIGHT-preAD study who are cognitively unimpaired individuals between 70 and 85 years old with subjective memory complaints. Network measures such as size of the network, average degree, path length, clustering coefficient, and betweenness centrality were calculated for every individual. In people with increased A β accumulation, lower small world levels (σ) were observed. Similar results were seen with A β levels and normalized clustering coefficient (γ) and normalized path length (λ).

Considering the relationship between regional network and A β changes, encountered an effect in the precuneus and orbitofrontal cortex which can be the regions of early A β accumulation. No effect of APOE ϵ 4 was found on association between A β accumulation and gray matter network measures. As stated by other studies and ten Kate et al (2018a) APOE ϵ 4 strongly affects A β accumulation but it does not particularly highlight the anatomical regions that will show most substantial structural brain changes (ten Kate et al., 2018a). Not only A β deposition but it is also hypothesized that tau deposition may contribute to changes in gray matter networks in AD pathology. One study measured tau PET to observe whether it is associated with gray matter network alterations across individuals across the AD continuum. For this aim, they looked at 533 individuals from Swedish BioFINDER study who are above 50 years of age and have abnormal CSF A β 42/40 ratio. Four groups were included in the study. Individuals that are A β positive and cognitively unimpaired, A β positive with MCI, A β positive with AD dementia and lastly the control group that are A β negative and cognitively unimpaired. To assess network properties network size, degree, connectivity density, clustering coefficient, path length, and the small world coefficient were calculated. They showed that higher the tau PET levels are linked to greater the gray matter network disruptions in individuals across the AD continuum. Tau deposition is related to decreased communication between brain areas and abnormalities in the brain regions that reveal more random network topology across AD pathology stages. All A β positive groups showed increased network abnormalities, the severity increased with advancing disease stage. MCI patients showed lower clustering, path length, and small world coefficient values compared to the control group. Additionally, people with AD had lower network size and degree compared to A β negative individuals. According to the

results, there may be a relationship between tau deposition and gray matter networks in individuals who are A β positive. Greater tau deposition was associated with increased randomly connected nodes. Individuals with AD dementia had more hindered gray matter network topology compared to MCI and A β positive cognitively unimpaired individuals (Pelkmans et al., 2021b).

According to previous literature by Dicks et al (2020), individuals with higher tau levels will show greater gray matter network disruptions. In one previous study changes in gray matter network measures within individuals across the AD continuum were examined. They observed if gray matter network measures are affected by tau deposition and if they show significant differences in specific cognitive domains. A total of 713 participants' data was used, including individuals who are cognitively unimpaired with normal A β levels (controls), as well as individuals with preclinical AD, prodromal AD (MCI) and ones that have dementia due to AD from Alzheimer's Disease Neuroimaging Initiative (ADNI) cohort. A β levels were determined according to both A β PiB PET or CSF A β 42 levels. For the network analysis, network size, degree, connectivity density, clustering coefficient, path length, and small world measure (sigma) were computed. Regarding gray matter network measures, individuals with AD dementia showed the lowest path length values compared to all the groups. Small world measures were highest for the control group and lowest for the AD dementia individuals. With time, network measures decreased except for the connectivity density in all groups. Decline in network measures were greater as the disease progressed. They used tau levels as normal and abnormal. A comparison was made between individuals with preclinical AD with and without having abnormal values of tau. Individuals with pathological levels of tau showed a sharper decline in small world measures. These results supported previous research on disrupted gray matter network measures across the AD spectrum. Results added a value to recent research as this study was done by using a longitudinal approach and supporting the finding of gray matter network restructuring towards a more random topology in older age as the disease progresses (Dicks et al., 2020).

Another study examined changes in gray matter networks due to tau deposition. They used CSF p-tau 181 levels to indicate abnormal tau deposition. They further investigated if the relationship between p-tau 181 levels and subject specific gray matter network disruptions were dependent on A β levels (CSF A β 42) and/or cognitive dementia rating (CDR) scale status. If an individual has a score of 0 from CDR this indicates no dementia and if they received 3 this refers to severe dementia. Data were gathered from European Prevention of Alzheimer's Dementia (EPAD) consisting of healthy individuals

without AD who are above 50 years old. They were either A β negative or A β positive, some individuals with CDR of 0 and the rest with CDR of 0.5. CSF, neuroimaging, and neuropsychological data were collected. They constructed network matrices to analyze changes in gray matter networks. Higher p-tau 181 levels were found in A β positive individuals compared to A β negative. Furthermore, A β positive individuals have lower network density, clustering coefficient, gamma and small world coefficient. They found higher p-tau 181 levels were associated with lower betweenness centrality, lambda, and path length. They observed that the relationship between tau deposition and changes in network metrics depended both on CDR and A β levels. They performed a three way interaction analysis with p-tau, A β status and CDR score on network properties. As hypothesized, a relationship was found between p-tau 181 and global network measures mediated by CDR score and A β status. Individuals who had impaired cognition with a CDR score of 0.5 who were also A β positive showed lower clustering coefficient in regard to higher p-tau 181 levels. A reduced clustering coefficient was found which may reflect local synaptic dysfunction due to early A β disruptions. They also observed higher path length values associated with lower A β 42 CSF levels which were not inline with similar past research. These observed inconsistencies in path length could be attributed to a non-linear pattern in how it changes throughout the disease progression. Initially, path length might increase due to the loss of local connections within the network. This rise reflects the heterogeneous pattern on tissue degeneration. However, in later stages of the disease, as the network becomes increasingly sparse with further connection loss, path length might eventually decrease. They identified lower betweenness centrality associated with higher p-tau. As a whole, the analysis of gray matter networks revealed disruptions that were linked to p-tau 181 levels. These disruptions exhibited distinct characteristics depending on the presence of A β plaques and the cognitive status of the individuals, suggesting that A β accumulation and tau deposition can have a combined effect leading to different patterns of early alterations in networks in preclinical stages (Luigi et al., 2022).

Study Aim

Identifying network disruptions is crucial to understand the connection between areas which are related to cognitive decline and disease progression. It is still unclear and complex at which time point during the development of AD, gray matter networks become disorganized (Tijms et al., 2016). To investigate the structural organization of gray matter networks and how they may change, previous studies have employed graph theoretical

analysis. These studies have identified alterations in brain network properties at both a global and regional level. In this thesis, also graph theoretical method was utilized to examine the relationship between different graph properties and biomarkers of CSF A β 42/40 ratio, CSF p-tau and different risk factors such as gender, APOE status, education and age in a preclinical AD cohort.

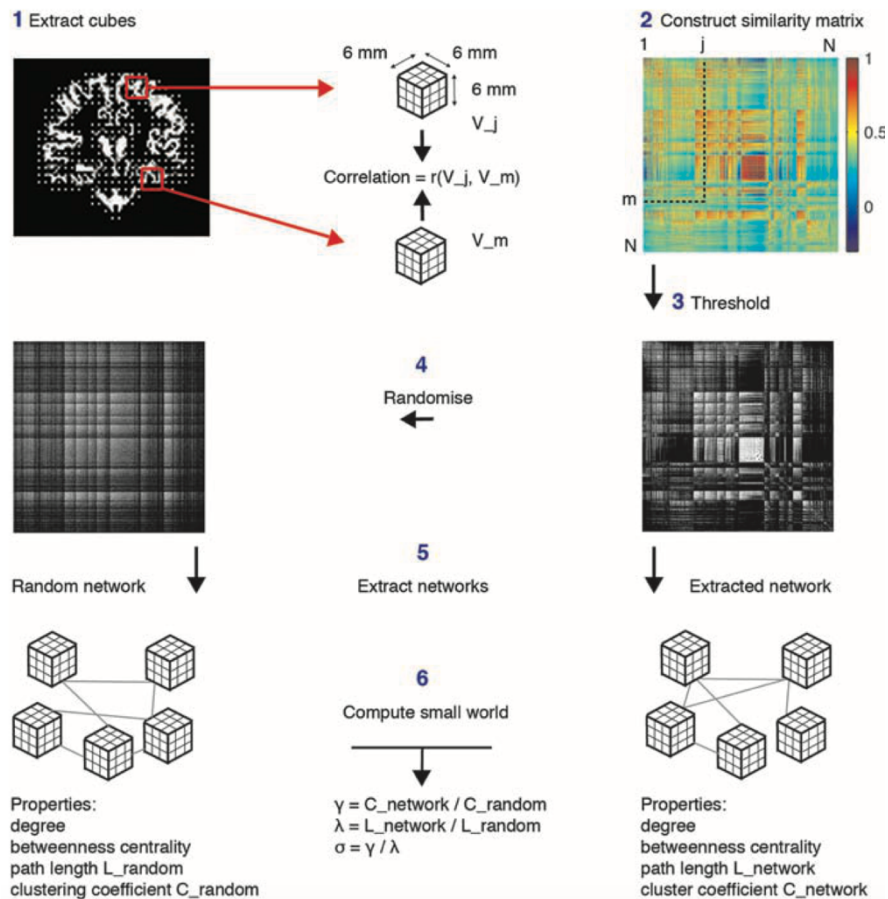
Materials and Methods

Single subject Gray Matter Network analysis

Previous studies have analyzed gray matter networks at the single subject level (*Figure 3*). Examining them individually can be useful for assessing individual differences in brain structure and capturing unique network architectures, revealing significant variability between individuals. By using a single subject gray matter network graph, the relationship between changes in graph properties and cognitive decline can be identified at both the general brain level and in regional analyses. Specific cortical regions, which are often highly interconnected and targeted by A β accumulation in AD, contribute more to disease severity.

The method used in this thesis for constructing individual networks was first employed by Tijms et al (2012 & 2013a&b). Initially, gray matter was segmented from T1 weighted MRI images, and the segmented gray matter was divided into 3x3x3 voxel cubes. The similarity between these cubes was computed, allowing the cortex to maintain its 3D structure and preserving information about local thickness and folding. A network was created when the structural similarity quantified by the correlation coefficient between two nodes, exceeded a certain threshold. Network metrics such as the degree, path length, clustering coefficient, small world properties and betweenness centrality were then computed (Tijms et al., 2012).

By using these single subject gray matter network graphs, it becomes possible to identify the relationship between graph property changes and biomarker progression both globally and regionally. This method highlights how specific cortical regions contribute to disease severity and how these regions targeted by A β and tau accumulation in AD exhibit unique network disruptions.



(Tijms et al., 2011) *Figure 3: Pipeline of the extraction of individual networks*

MATLAB Script Explanation

T1 images for each participant were obtained from the Alfa + cohort and segmented using SPM12. The images were segmented into gray matter, white matter, and CSF. These segmented brain scans were transformed into the standard MNI space based on the deformation fields. The forward deformation field was used to warp the subject's scan to the MNI space, while the inverse deformation field allowed data to be warped back to the subject's native space.

In the next step, cubes were created from the gray matter segmentation, with the MRI image dimensions 91x109x91 voxels defined for network conversion. Each cube was set to a size of 3x3x3 voxels. To extract networks, the gray matter image was co-registered with the T1 image to ensure alignment in MNI space. For data reduction, the co-registered gray matter image was resliced into a standard voxel size of 2x2x2 mm. A template was then used to extract the minimum number of cubes from the scan. Voxel indices belonging to each cube were loaded. A randomized brain was created to be used in a later analysis when

estimating a threshold for correlation analysis. Correlation matrices were extracted between the original and randomized network data. A threshold was determined to distinguish significant correlations from noise in the original network data. A binary matrix was created to set all correlation values above the threshold to 1 which indicates that there is a connection and all values below the threshold to 0 which refers to no connection. Weak and nonexistent connections were removed, and the number of connections (degree) for each cube was calculated. The network was checked for any disconnected nodes; if none were found, graph theory matrices such as connectivity density, average clustering, average path length, average betweenness centrality, gamma, lambda, and sigma were computed. Additionally, five random networks with the same degree distribution were generated to compare the small world properties of the original network. Network property values were calculated for each subject, and these values were compiled into a data table for subsequent analysis.

For regional analysis, some graph measures were extracted from the Automated Anatomical Labeling (AAL) atlas for each subject. First, a SPM batch script was used to warp the atlas to the subject space, reorienting it to match the gray matter image orientation. Later, the atlas was resliced and masked with the resliced gray matter image. Regional volumes were calculated based on the gray matter image information. In the end, network properties were gathered for each AAL region for each subject. The MATLAB script used in this thesis is available at [GitHub](#).

Participants

The Alfa + cohort is a nested long term longitudinal study derived from the Alfa (for Alzheimer and Families) project, comprising the Alfa parent cohort and the nested Alfa + cohort. The Alfa cohort includes cognitively unimpaired subjects aged between 45 and 74 years, who undergo cognitive testing, clinical history assessments and blood samples collection. This Alfa parent cohort serves as the foundation for future studies. A subgroup of participants from the Alfa parent cohort was invited to join the Alfa + study which aims to understand early pathophysiological changes in AD during its preclinical stage. Inclusion criteria for this cohort required participants to be cognitively healthy, Spanish and/or Catalan speakers aged 45 to 74 years. Exclusion criteria were having cognitive performance outside of the established cutoff for specific tests (Mini Mental State Examination, MMSE, <26; Memory Impairment Screen, MIS, <6; Time Orientation Subtest of Barcelona test II, <68; Semantic fluency test animals, <12; Clinical Dementia Rating Scale, CDR, >0). Individuals

with major psychiatric disorders, neurological disorders, brain injuries affecting normal cognitive abilities and a family history of AD with a suspected autosomal dominant pattern were also excluded. In addition to the measures collected from the parent cohort, the Alfa + cohort participants provided biomarkers such as CSF (A β 40, A β 42, p-tau, t-tau), urine samples, blood (APOE status), MRI (T1, T2, flair, resting state fMRI sequences) and PET (FDG, A β , tau) scans. Participants were selected based on their risk profiles, including APOE levels and family history status. The cohort consists of 400 participants with follow ups every three years, although this number may change due to updated inclusion criteria or participation attrition.

The Alfa study protocol was approved by the Independent Ethics Committee at Parc de Salut de Mar Barcelona. All participants provided informed consent by signing a consent form. Furthermore, each participant had a close relative who volunteered for functional assessment protocol, and their consent was also acquired.

This thesis includes data from 362 participants from the baseline session of the Alfa + cohort. High resolution MRI scans were conducted at Barcelona β eta Brain Research Center using Philips Ingenia CX 3T MRI scanner with T1 images used for analysis. One participant was excluded from the analysis due to an abnormally high level of p-tau.

Statistical Analysis

For the sample description, the mean values and standard deviations of APOE status, AT status, p-tau levels and network measures were calculated. To analyze the relationship between CSF A β 42/40 ratio and CSF p-tau levels with different network properties, the first general linear model was created which was adjusted for APOE status, age, sex, education years, and size of the networks. The second model was generated to see whether there was an interaction effect of different APOE groups (individuals with no carriers of APOE ϵ 4, individuals with only one allele of APOE ϵ 4 and people with two alleles of APOE ϵ 4) on the association between CSF A β 42/40 ratio and network measures. This association was also observed between CSF p-tau and network measures in the third model. With the fourth model, the interaction effect of different AT groups (A-T- / A+T- / A+T+) on the association between CSF A β 42/40 ratio and network properties was observed. This analysis was repeated by replacing A β with CSF p-tau in the fifth model. For the last model, the whole brain analysis relationship between CSF A β 42/40 ratio and CSF p-tau levels and global gray matter network measures was observed in different AT groups.

To explore the relationship between CSF A β 42/40 ratio and CSF p-tau levels on regional network property measures, 116 regions of AAL atlas were used for the analysis. The regional analysis was performed on four network properties which are average path length, average degree, average betweenness centrality, and average clustering. For each network property two tables were constructed, one to assess the association of regional network property values with CSF A β 42/40 ratio and the second one to assess the relationship of regional graph property values with p-tau levels. In the end eight general linear models were computed. Both for global and regional analysis Rstudio was used.

Results

Subjects

Participants (n=362) had an average age of 60.8 years, 59% of them were females. The average years of education was 13 years. Majority of the participants (44.8%) did not carry the gene APOE ϵ 4, while 43.6% carried only one allele of ϵ 4 and 8.5% of them had both ϵ 4 alleles. 215 subjects were A β and tau negative, 88 of them were only A β positive and 28 of them were both A β and tau positive. This low number for A+T+ positive group can be explained due to the nature of the cohort since it contains preclinical AD individuals.

Table 1 Characteristics of Alfa + cohort Participants

Demographics	Sample=362
Female sex (%)	214 (59.12)
Age (sd)	60.8 (4.73)
Years of education (sd)	13.6 (3.53)
Genetic	
APOE- ϵ 2/ ϵ 3 & ϵ 3/ ϵ 3 (%)	163 (44.75)
APOE- ϵ 3/ ϵ 4 (%)	158 (43.64)
APOE- ϵ 4/ ϵ 4(%)	32 (8.48)
Biomarkers	
A-T- (%)	215 (59.29)
A+T- (%)	88 (24.31)
A+T+ (%)	28 (7.73)

Table 2 Characteristics of Network Properties for total sample and for 3 AT groups

Network Properties	Sample=362	A-T- (%)	A+T- (%)	A+T+ (%)
Network size (sd)	6872.66 (623.86)	6842.1 (608.19)	6999.83 (597.69)	6708.39 (783.18)
Average degree (sd)	1125.75 (130.80)	1127.17 (126.99)	1133.01 (123.58)	1091.88 (169.91)
Connectivity density (sd)	16.37 (1.07)	16.47 (1.05)	16.19 (1.22)	16.23 (1.10)
Average clustering (sd)	0.49 (0.02)	0.47 (0.02)	0.47 (0.02)	0.47 (0.02)
Average path length (sd)	2.03 (0.03)	2.03 (0.03)	2.04 (0.03)	2.04 (0.02)
Average betweenness centrality (sd)	7093.68 (623.73)	7044.86 (609.14)	7250.17 (603.93)	6947.85 (767.30)
Gamma (sd)	1.72 (0.09)	1.71 (0.10)	1.73 (0.18)	1.72 (0.19)
Lambda (sd)	1.11 (0.01)	1.12 (0.01)	1.11 (0.01)	1.11 (0.01)
Sigma (sd)	1.55 (0.06)	1.55 (0.07)	1.56 (0.06)	1.55 (0.07)
Disconnected nodes (sd)	0 (0)	0 (0)	0 (0)	0 (0)

Global Analysis

Relationship between CSF A β 42/40 ratio and CSF p-tau levels and global gray matter network measures in whole group

No significant association was found between CSF A β 42/40 and whole brain network properties. However, relationships were observed between network properties such as average path length, average betweenness centrality, gamma, lambda, sigma and CSF p-tau levels, showing the main effect of p-tau on network measures. Average path length had a positive significant relationship with p-tau (beta=3.021e-02, t-value=3.362, p=0.001 (df = 335)). Higher p-tau levels were also associated to other network properties such as average betweenness centrality (beta=211.80943, t-value=3.371, p=0.001 (df = 335)), gamma (beta=9.852e-02, t-value=3.653, p=0.0003 (df = 335)), lambda (beta=1.408e-02, t-

Investigating Gray Matter Network Alterations in Preclinical Alzheimer's Disease 27 Using Graph Theoretical Measures

value=3.728, $p=0.0002$ (df = 335)), sigma (beta=6.985e-02, t-value=3.531, $p=0.0005$ (df = 335)). No significant association was found between p-tau levels and network matrices of average degree, connectivity density, and average clustering.

Table 3 Network Properties with Significant Relationship with p-tau

Network properties	β	t-value	p-value (0.05)
Average path length	3.021e-02	3.362	0.001
Average betweenness centrality	211.80943	3.371	0.001
centrality			
Gamma	9.852e-02	3.653	0.0003
Lambda	1.408e-02	3.728	0.0002
Sigma	6.985e-02	3.531	0.0005

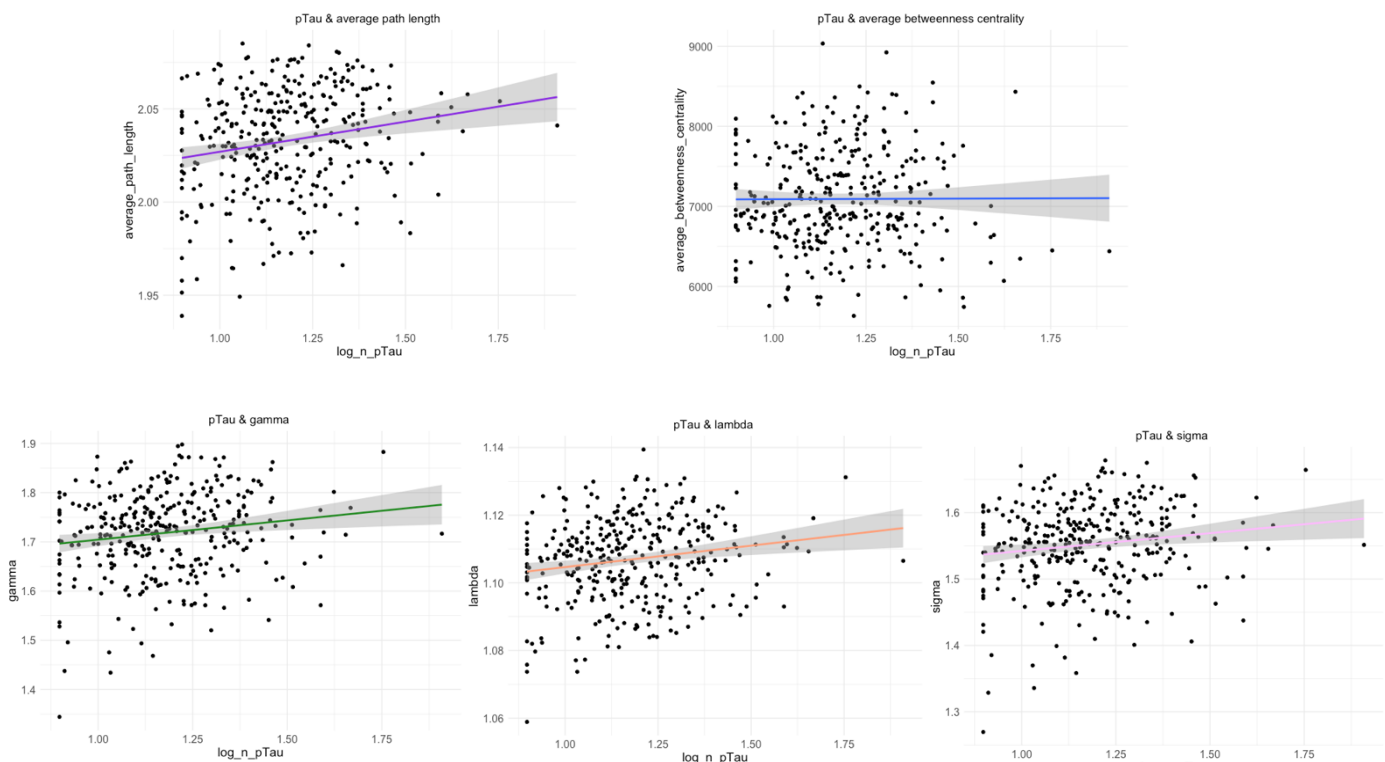


Figure 4 Network Properties with Significant Relationship with p-tau

Interaction Models

No interaction effects were found on AT groups on the relationship between A β 42/40 and graph property values. As well as the relationship between p-tau levels and network property values was not influenced by AT groups. Similarly to the AT groups there

was no significant interaction between APOE groups and A β 42/40 on network properties. APOE groups did not moderate the relationship between p-tau levels and network property values.

Main effects of sex and age on global gray matter network measures

Moreover, significant relationships were found between some network properties and age and sex. Female sex showed higher graph property values compared to males in average path length (beta=1.369e-02, t-value=3.46, p=0.001 (df = 335)), average betweenness centrality (beta=97.68, t-value=3.53, p=0.0005 (df = 335)), gamma (beta=4.900e-02, t-value=4.13, p=<0.001 (df = 335)), lambda (beta=7.860e-03, t-value=4.73, p=<0.001 (df = 335)), and sigma (beta=3.335e-02, t-value=3.83, p=0.0001 (df = 335)).

Age had a significant impact on some network properties. The older the age, the lower the average degree (beta=-3.26, t-value=-3.63, p=0.0003 (df = 335)), connectivity density (beta=-0.05, t-value=-3.64, p=0.0003 (df = 335)), average clustering (beta=-1.059e-03, t-value=-4.75, p=<0.001 (df = 335)), gamma (beta=-4.742e-03, t-value=-4.76, p=<0.001 (df = 335)), lambda (beta=-4.782e-04, t-value=-3.43, p=<0.001 (df = 335)), and sigma (beta=-3.629e-03, t-value=4.97, p=<0.001 (df = 335)).

Table 4 Network Properties with Significant Relationship with sex

Network properties	β	t-value	p-value (0.05)
Average path length	1.369e-02	3.46	0.001
Average betweenness centrality	97.68	3.53	0.0005
Gamma	4.900e-02	4.13	<0.001
Lambda	7.860e-03	4.73	<0.001
Sigma	3.335e-02	4.97	<0.001

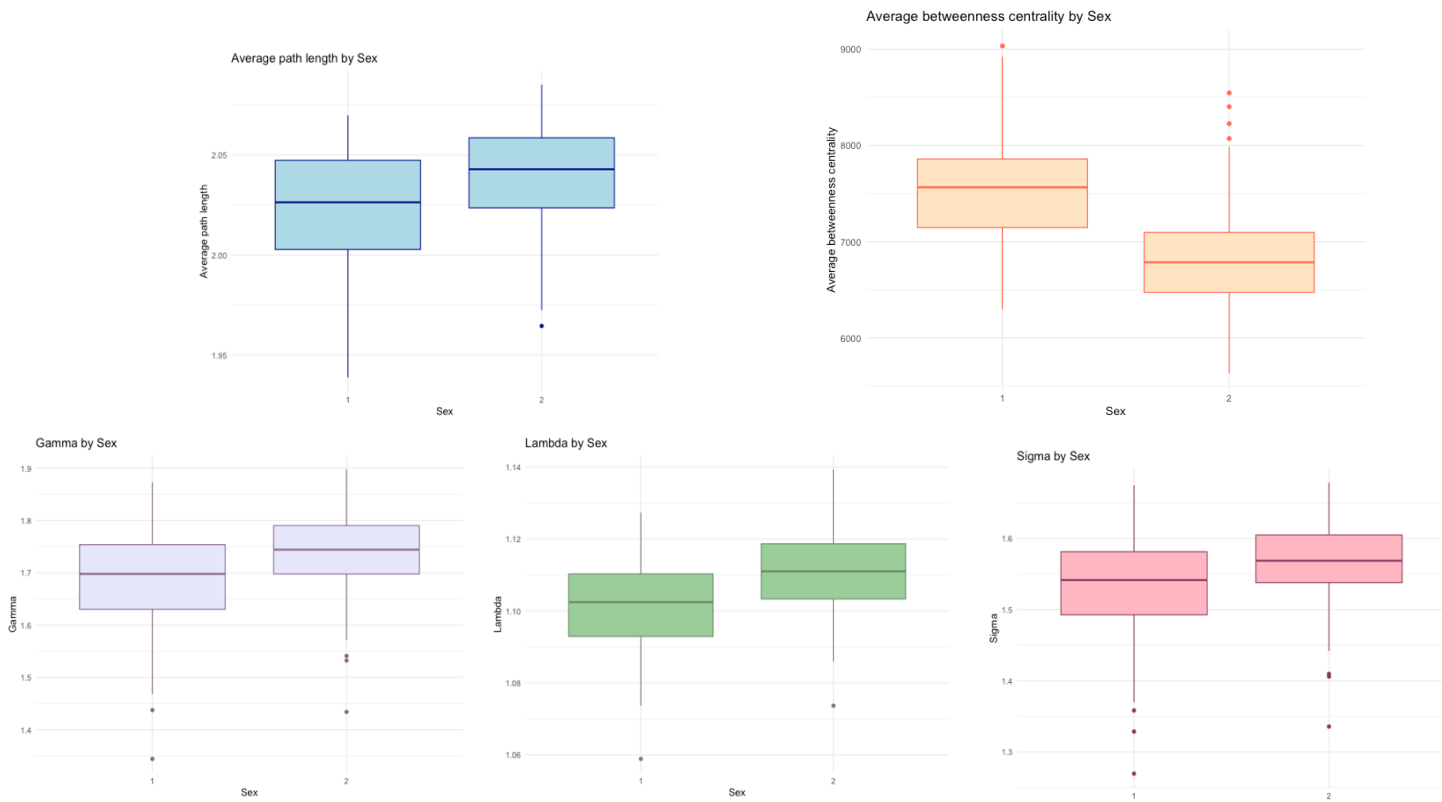


Figure 5 Network Properties with Significant Relationship with sex

Table 5 Network Properties with Significant Relationship with age

<u>Network properties</u>	<u>β</u>	<u>t-value</u>	<u>p-value (0.05)</u>
Average degree	-3.26	-3.63	0.0003
Connectivity density	-0.05	-3.64	0.0003
Average clustering	-1.059e-03	-4.75	<0.001
Gamma	-4.742e-03	-4.76	<0.001
Lambda	-4.782e-04	-3.43	<0.001
Sigma	-3.629e-03	4.97	<0.001

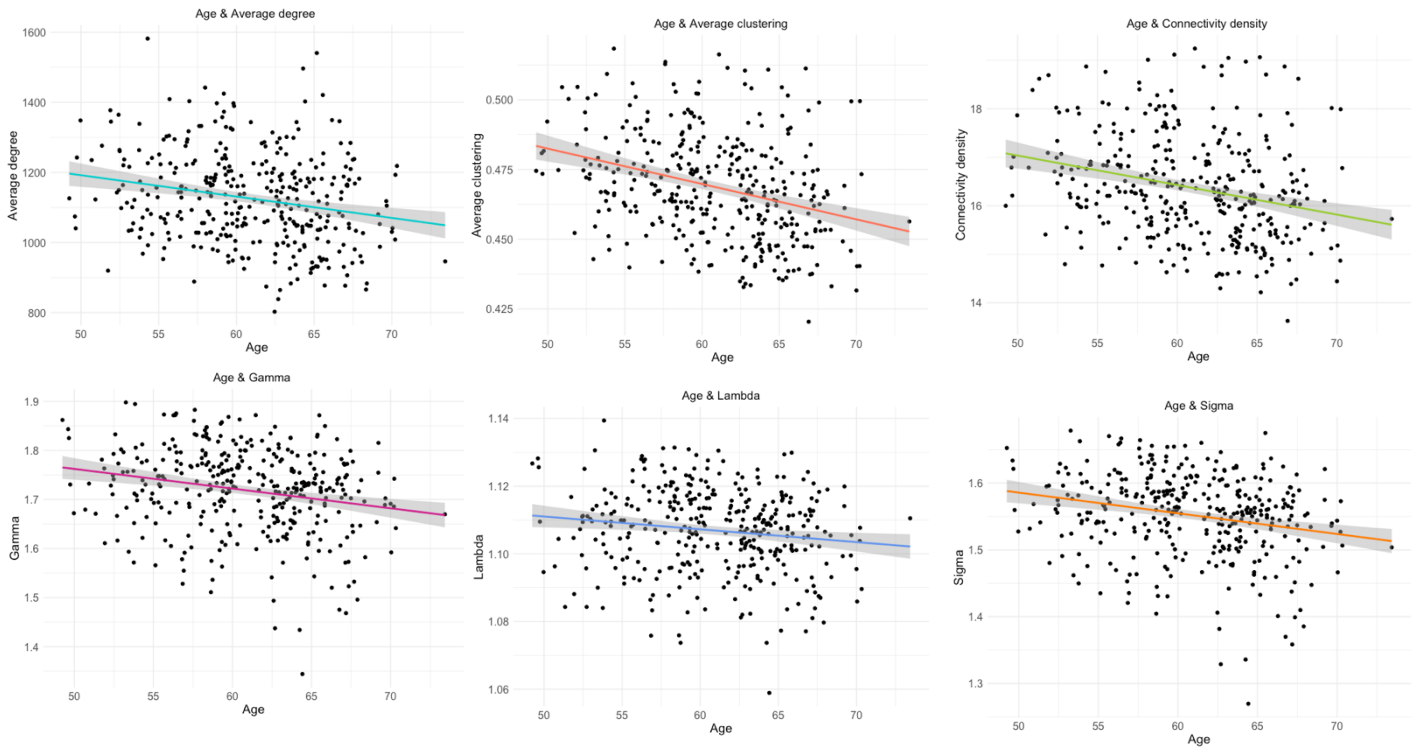


Figure 6 Network Properties with Significant Relationship with age

Relationship between CSF A β 42/40 ratio and CSF p-tau levels and global gray matter network measures in different AT groups

No significant association was examined between CSF A β 42/40 and whole brain network properties for all the AT groups. Significant positive association was observed between CSF p-tau and network properties of average path length ($\beta=3.390e-02$, t -value=2.032, $p=0.04$), average betweenness centrality ($\beta=253.09817$, t -value=2.175, $p=0.03$), gamma ($\beta=253.09817$, t -value=2.175, $p=0.03$), lambda ($\beta=1.524e-02$, t -value=2.122, $p=0.04$), sigma ($\beta=9.668e-02$, t -value=2.647, $p=0.009$) in group A-T-. No significant relationship was seen for any of the network properties and p-tau for the A+T- group. Only for one network property which is average clustering, p-tau had a positive significant relationship ($\beta=7.096e-02$, t -value=2.141, $p=0.04$) in group A+T+.

Regional Analysis

Relationship between CSF A β 42/40 ratio and regional gray matter network measures

The relationship between average betweenness centrality and A β 42/40 ratio were significant in three regions; superior frontal gyrus left ($\beta=-6167$, standard-error=1914, $p=0.001$), superior frontal gyrus right ($\beta=-4386$, standard-error=2049, $p=0.03$) and left

precuneus (beta=-5802, standard-error=2627 p=0.02) before correction for multiple testing. The direction of the relationship was negative for all the regions. However, after the false discovery rate (FDR) correction, none of the regions had significant association between betweenness centrality and Aβ42/40 ratio (p-values respectively: 0.16, 0.76, 0.76).

The association between average clustering and Aβ42/40 ratio were positive and significant in four regions, right precentral gyrus (beta=0.17, standard-error=0.08 p=0.04), left frontal gyrus medial orbital (beta=0.28, standard-error=0.14 p=0.04), right paracentral lobule (beta=0.27, standard-error=0.13 p=0.04) and left lobule 9 of cerebellar hemisphere (beta=0.22, standard-error=0.10 p=0.04) before the FDR correction. The regions were not significant after the multiple testing correction with all having p-value of 0.8.

We then examined the relationship between average path length and Aβ42/40 ratio. This relationship was significant in the left precentral gyrus (beta=-0.18, standard-error=0.08 p=0.02), left rolandic operculum (beta=-0.29, standard-error=0.14 p=0.03), left insula (beta=-0.17, standard-error=0.18 p=0.01), left supramarginal gyrus (beta=-0.34, standard-error=0.12 p=0.003), right paracentral lobule (beta=-0.28, standard-error=0.13p=0.03), and right temporal pole:middle temporal gyrus (beta=-0.31, standard-error=0.14 p=0.03) regions. After the correction for multiple testing, none of the p-values were significant, the p-values are displayed respectively: 0.43, 0.43, 0.40, 0.21, 0.43, 0.43.

The association between average degree and Aβ42/40 ratio was significant in the positive direction for only one region which is left supramarginal gyrus (beta=1012, standard-error=437 p=0.02). This association was not significant after the FDR correction (p-value=0.82=).

Table 6 Relationship between CSF Aβ42/40 ratio and regional gray matter network measures

Network properties	β	Standard error	p-value	Corrected p-value
Average betweenness centrality				
Superior frontal gyrus left	-6167	1914	0.001	0.16
Superior frontal gyrus right	-4386	2049	0.03	0.76
Left precuneus	-5802	2627	0.02	0.76
Average clustering				
Right precentral gyrus	0.17	0.08	0.04	0.8
Left frontal gyrus medial orbital	0.28	0.14	0.04	0.8

Right paracentral lobule	0.27	0.13	0.04	0.8
Left lobule 9 of cerebellar hemisphere	0.22	0.10	0.04	0.8
Average path length				
Left precentral gyrus	-0.18	0.08	0.02	0.43
Left rolandic operculum	-0.29	0.14	0.03	0.43
Left insula	-0.17	0.18	0.01	0.40
Left supramarginal gyrus	-0.34	0.12	0.003	0.21
Right paracentral lobule	-0.28	0.13	0.03	0.43
Right temporal pole:middle temporal gyrus	-0.31	0.14	0.03	0.43
Average degree				
Left supramarginal gyrus	1012	437	0.02	0.82

Relationship between CSF p-tau levels and regional gray matter network measures

The link between average betweenness centrality and p-tau levels was significant in left superior frontal gyrus orbital (beta=1349, standard-error=385 p=0.001), right superior frontal gyrus orbital (beta=960, standard-error=418 p=0.02), right inferior frontal gyrus orbital (beta=703, standard-error=305 p=0.02), right rolandic operculum (beta=874, standard-error=286 p=0.002), right insula (beta=-927, standard-error=445 p=0.03), and right calcarine sulcus (beta=584, standard-error=297 p=0.049). Of these regions only the left superior frontal gyrus orbital showed a significant association after being corrected for multiple testing (p-value=0.02).

The association between average clustering and p-tau levels was significant in regions left rolandic operculum (beta=0.03, standard-error=0.01 p=0.03), left angular gyrus (beta=0.03, standard-error=0.01 p=0.047), right Heschl's gyrus (beta=-0.05, standard-error=0.02 p=0.01), right lobule 8 of cerebellar hemisphere (beta=0.02, standard-error=0.01 p=0.03), left lobule 10 of cerebellar hemisphere (beta=0.15, standard-error=0.07 p=0.04), and lobule 1-2 of vermis (beta=0.14, standard-error=0.36 p=0.0002). Following the correction, only lobule 1-2 of vermis displayed a significant association (p-value=0.03).

The relationship between average path length and p-tau levels was statistically significant in the left superior frontal gyrus (beta=0.03, standard-error=0.01 p=0.01), left middle frontal gyrus (beta=0.02, standard-error=0.01 p=0.01), right middle frontal gyrus

(beta=0.02, standard-error=0.01 p=0.03), right inferior frontal gyrus opercular part (beta=0.04, standard-error=0.01 p=0.001), right inferior frontal gyrus triangular part (beta=0.03, standard-error=0.01 p=0.004), and left insula (beta=0.05, standard-error=0.02 p=0.01). None of the regions had significant association after the correction (p-values respectively: 0.14, 0.14, 0.24, 0.09, 0.12, 0.14).

The network property of average degree and p-tau levels showed significant association in areas such as left superior frontal gyrus orbital (beta=168, standard-error=55.9 p=0.002), left rolandic operculum (beta=111, standard-error=52.7 p=0.04), right fusiform gyrus (beta=99.4, standard-error=40.1 p=0.01), left angular gyrus (beta=119, standard-error=49.3 p=0.02), right angular gyrus (beta=91.8, standard-error=45.7 p=0.045), and left paracentral lobule (beta=-150, standard-error=60.3 p=0.01). After the correction for multiple testing, there were no significant regions.

Table 7 Relationship between CSF p-tau levels and regional gray matter network measures

Network properties	β	Standard error	p-value	Corrected p-value	
Average betweenness centrality					
Left superior frontal gyrus orbital	1349	385	0.001	0.02	*
Right superior frontal gyrus orbital	960	418	0.02	0.19	
Right inferior frontal gyrus orbital	703	305	0.02	0.19	
Right rolandic operculum	874	286	0.002	0.055	
Right insula	-927	445	0.03	0.25	
Right calcarine sulcus	584	297	0.049	0.28	
Average clustering					
Left rolandic operculum	0.03	0.01	0.03	0.90	
Left angular gyrus	0.03	0.01	0.047	0.92	
Right Heschl's gyrus	-0.05	0.02	0.01	0.78	
Right lobule 8 of cerebellar hemisphere	0.02	0.01	0.03	0.90	
Left lobule 10 of cerebellar hemisphere	0.15	0.07	0.04	0.90	

Lobule 1-2 of vermis	0.14	0.36	0.0002	0.03	*
Average path length					
Left superior frontal gyrus	0.03	0.01	0.01	0.14	
left middle frontal gyrus	0.02	0.01	0.01	0.14	
Right middle frontal gyrus	0.02	0.01	0.03	0.24	
Right inferior frontal gyrus opercular part	0.04	0.01	0.001	0.09	
Right inferior frontal gyrus triangular part	0.03	0.01	0.004	0.12	
Left insula	0.05	0.02	0.01	0.14	
Average degree					
Left superior frontal gyrus orbital	168	55.9	0.002	0.14	
Left rolandic operculum	111	52.7	0.04)	0.47	
Right fusiform gyrus	99.4	40.1	0.01	0.31	
Left angular gyrus	119	49.3	0.02	0.31	
Right angular gyrus	91.8	45.7	0.045	0.48	
Left paracentral lobule	-150	60.3	0.01	0.31	

Discussion

This thesis investigated the association between gray matter network matrices by using graph theoretical approach and AD biomarkers CSF A β 42/40 ratio, CSF p-tau in cognitively healthy individuals. No significant relationship of A β 42/40 on network properties was found. This can be explained by the fact that the investigated cohort did not show any clinical symptoms. Even considering different AT groups, no significant differences were found between the groups regarding the effects of A β on network properties.

According to the findings, for all the subjects in the global brain analysis, when p-tau levels were increased average path length, average betweenness centrality, gamma, lambda and sigma were increased as well. Average path length measures the shortest distance between nodes in a network. A shorter average path length indicates more efficient information flow. As displayed in the results, increased p-tau levels lead to slower and less efficient connections, resulting in a increased average path length. While betweenness centrality typically decreases in AD, our study found an opposite result in this cohort. This

might suggest that certain brain regions such as hubs (high betweenness centrality) can appear to be stable and resilient against AD. These results can suggest that gray matter alterations can be related to early pathological changes in AD, which can be detected from early on in cognitively healthy individuals.

Changes in small world property can be an early sign of network disruptions due to AD such as A β and tau, so it is useful to benefit from this as a biomarker and monitor disease progression. Healthy individuals have a well structured network organization, often described as a small world network organization. In contrast, when it comes to AD the network appears to be more random and disorganized. Previous research have found that individuals that are in AD continuum have decreased small world property, suggesting a more random organization of the brain (Tijms et al., 2013a & 2018, ten Kate et al., 2018, Pelkmans et al., 2021b). In this work, a significant positive association was found between increasing p-tau and path length values. This contradiction between results can be due to the compensatory mechanisms in response to the pathological process occurring. Brain networks may reorganize themselves to maintain efficiency and functionality despite the pathological burden. This reorganization could lead to a temporary increase in small world property. Increased small world property might indicate that certain regions are becoming more efficient in their local connectivity. The relationship between the amount and the spread of tau accumulation and small world property can be complex and non-linear. Decrease in small world property can be seen as the disease progresses. In other studies the data was derived from further staging in disease continuum.

Similar contradictory results were found for both global path length and betweenness centrality. We found significant positive relationship between CSF p-tau levels and both path length and betweenness centrality. However previous research concluded both higher CSF p-tau and increased tau PET lead to lower path length (Pelkmans et al., 2021b; Luigi et al 2022). This discrepancy between the results can again be due to the compensatory mechanisms in the brain. As the disease progresses and neuronal damage becomes more widespread, these compensatory mechanisms may fail, resulting in a decrease in path length and betweenness centrality.

For the regional analysis, a relationship between four network properties and CSF A β and p-tau was observed. Some regions were significant before the correction which are known regions of A β deposition. Since in the global analysis none of the network properties showed a significant association, previous research considering the cortical A β staging model has shown that regional abnormality occurs before global positivity (Alchera et al.,

2023). None of the 116 regions were significant after multiple testing when looking at the relationship between CSF A β 42/40 ratio and regional gray matter network measures. Since there are many regions it is reasonable to not have significant relationships after the correction. It can also be the case that A β accumulation may have a more pronounced effect in regions that are not included in the analysis specifically, or the relationship might be more detectable when considering broader network level properties rather than individual regions.

Considering the relationship with p-tau, there was a significant relationship with betweenness centrality in left superior frontal gyrus orbital after the correction. The superior frontal gyrus includes the medial prefrontal cortex which is a part of the DMN. It is involved in higher order cognitive functions such as planning, decision making, working memory. Betweenness centrality reflects nodes that are more centrally connected relative to other nodes in the network which creates a hub. Hub regions are targeted more by AD as well as DMN regions. It means that superior frontal gyrus plays a crucial role in information processing and communication in individuals with AD, and this may explain some part of cognitive deficits observed in AD (Buckner et al., 2009). While in average clustering lobule 1-2 of vermis was significant. The significant role of the cerebellum in the neurobiology and symptomatology of AD helps explain our findings. Structural and functional cerebellar changes may impact behaviors and cognition in early stages of AD. The patterns of cognitive deficits can provide evidence for a modulating role of the cerebellum in the earliest stages. While the cerebellum is associated with motor control and coordination, its relationship to the clustering coefficient suggests that neurons in this region are highly interconnected, making it potentially vulnerable to AD (Jacobs et al., 2018).

It is important to be aware of the limitations and challenges that emerged in this study. Alfa + is a longitudinal cohort, in this study only information from the baseline visit has been used. For future research it will be beneficial to analyze patient data from the second and the third visit and observe where they stand in the continuum. In this study we used the AAL atlas comprised of 116 regions. However regions where A β and tau deposition occur are different than the regions of AAL so this may have attenuated some results. Moreover, due to sample characteristics since all the participants were cognitively unimpaired only a few of them had tau deposition. Since this is a single subject analysis, computations were done in native space to keep individual variability intact. Consequently, the number of nodes per subject was not constant.

Nonetheless the current research is valuable. Using graph theory properties we have the chance to examine gray matter network changes which are important for symptom onset

in individuals with preclinical AD without any cognitive impairments. These graph properties also have a big impact on tracking disease severity which can be important for new therapeutic approaches. By using the single subject method we can capture unique network architecture. Since there is no temporal information in single subject design there is also no variability within the subject. Future research can examine a longitudinal cohort with multiple visits, to further investigate changes in gray matter networks and their relationship to cognitive decline over time, providing insights into a symptom severity.

In conclusion, our findings suggest early gray matter network disruptions in relationship with CSF p-tau level but not with A β 42/40 ratio. With increasing CSF p-tau levels network organization becomes more random in preclinical AD.

References

- Alchera, N., Garibotto, V., Tomczyk, S., Treyer, V., Hock, C., Gietl, A. F., Lövblad, K., Scheffler, M., Chincarini, A., Frisoni, G. B., & Ribaldi, F. (2023). Patterns of amyloid accumulation in amyloid-negative cases. *Neurobiology of Aging*, *129*, 99–108. <https://doi.org/10.1016/j.neurobiolaging.2023.05.006>
- Alexander, G. E., Bergfield, K. L., Chen, K., Reiman, E. M., Hanson, K. D., Lin, L., Bandy, D., Caselli, R. J., & Moeller, J. R. (2012). Gray matter network associated with risk for Alzheimer's disease in young to middle-aged adults. *Neurobiology of Aging*, *33*(12), 2723–2732. <https://doi.org/10.1016/j.neurobiolaging.2012.01.014>
- Buckner, R. L., Sepulcre, J., Talukdar, T., Krienen, F. M., Liu, H., Hedden, T., Andrews-Hanna, J. R., Sperling, R. A., & Johnson, K. A. (2009). Cortical hubs revealed by intrinsic functional connectivity: mapping, assessment of stability, and relation to Alzheimer's disease. *Journal of Neuroscience*, *29*(6), 1860–1873. <https://doi.org/10.1523/jneurosci.5062-08.2009>
- Bullmore, E., & Sporns, O. (2009). Complex brain networks: graph theoretical analysis of structural and functional systems. *Nature Reviews Neuroscience*, *10*(3), 186–198. <https://doi.org/10.1038/nrn2575>
- Budelier, M. M., & Bateman, R. J. (2019). Biomarkers of Alzheimer Disease. *The Journal of Applied Laboratory Medicine*, *5*(1), 194–208. <https://doi.org/10.1373/jalm.2019.030080>
- Dubois, B., Feldman, H. H., Jacova, C., Cummings, J. L., DeKosky, S. T., Barberger-Gateau, P., Delacourte, A., Frisoni, G., Fox, N. C., Galasko, D., Gauthier, S., Hampel, H., Jicha, G. A., Meguro, K., O'Brien, J., Pasquier, F., Robert, P., Rossor, M., Salloway, S., & Sarazin, M. (2010). Revising the definition of Alzheimer's disease: a new lexicon. *The Lancet Neurology*, *9*(11), 1118–1127. [https://doi.org/10.1016/s1474-4422\(10\)70223-4](https://doi.org/10.1016/s1474-4422(10)70223-4)
- Dai, Z., & He, Y. (2014). Disrupted structural and functional brain connectomes in mild cognitive impairment and Alzheimer's disease. *Neuroscience Bulletin*, *30*(2), 217–232. <https://doi.org/10.1007/s12264-013-1421-0>

- Dicks, E., Vermunt, L., Van Der Flier, W. M., Barkhof, F., Scheltens, P., & Tijms, B. M. (2020). Grey matter network trajectories across the Alzheimer's disease continuum and relation to cognition. *Brain Communications*, 2(2). <https://doi.org/10.1093/braincomms/fcaa177>
- Ewers, M., Sperling, R. A., Klunk, W. E., Weiner, M. W., & Hampel, H. (2011). Neuroimaging markers for the prediction and early diagnosis of Alzheimer's disease dementia. *Trends in Neurosciences*, 34(8), 430–442. <https://doi.org/10.1016/j.tins.2011.05.005>
- He, Y., Chen, Z., & Evans, A. (2008). Structural Insights into Aberrant Topological Patterns of Large-Scale Cortical Networks in Alzheimer's Disease. *Journal of Neuroscience*, 28(18), 4756–4766. <https://doi.org/10.1523/jneurosci.0141-08.2008>
- Hedden, T., Van Dijk, K. R. A., Becker, J. A., Mehta, A., Sperling, R. A., Johnson, K. A., & Buckner, R. L. (2009). Disruption of functional connectivity in clinically normal older adults harboring amyloid burden. *The Journal of Neuroscience: The Official Journal of the Society for Neuroscience*, 29(40), 12686–12694. <https://doi.org/10.1523/JNEUROSCI.3189-09.2009>
- Hansson, O. (2021). Biomarkers for neurodegenerative diseases. *Nature Medicine*, 27(6), 954–963. <https://doi.org/10.1038/s41591-021-01382-x>
- Jack, C. R., Knopman, D. S., Jagust, W. J., Shaw, L. M., Aisen, P. S., Weiner, M. W., Petersen, R. C., & Trojanowski, J. Q. (2010). Hypothetical model of dynamic biomarkers of the Alzheimer's pathological cascade. *The Lancet Neurology*, 9(1), 119–128. [https://doi.org/10.1016/s1474-4422\(09\)70299-6](https://doi.org/10.1016/s1474-4422(09)70299-6)
- Jack, C. R., Bennett, D. A., Blennow, K., Carrillo, M. C., Feldman, H. H., Frisoni, G. B., Hampel, H., Jagust, W. J., Johnson, K. A., Knopman, D. S., Petersen, R. C., Scheltens, P., Sperling, R. A., & Dubois, B. (2016). A/T/N: An unbiased descriptive classification scheme for Alzheimer disease biomarkers. *Neurology*, 87(5), 539–547. <https://doi.org/10.1212/wnl.0000000000002923>

- John, M., Ikuta, T., & Ferbinteanu, J. (2017). Graph analysis of structural brain networks in Alzheimer's disease: beyond small world properties. *Brain Structure & Function*, 222(2), 923–942. <https://doi.org/10.1007/s00429-016-1255-4>
- Jacobs, H. I. L., Hopkins, D. A., Mayrhofer, H. C., Bruner, E., Van Leeuwen, F. W., Raaijmakers, W., & Schmahmann, J. D. (2017). The cerebellum in Alzheimer's disease: evaluating its role in cognitive decline. *Brain*, 141(1), 37–47. <https://doi.org/10.1093/brain/awx194>
- Love, S., Budka, H., Ironside, J. W., Perry, A. (2014) *Greenfield's Neuropathology*. CRC Press
- Luigi, L., Silvia, I., Viktor, W., Wink, A. M., Mutsaerts, H. J., Sven, H., Kaj, B., O'Brien, J. T., Giovanni, F. B., Gael, C., Pierre, P., Pablo, M.-L., Adam, W., Joanna, W., Craig, R., Gispert, J. D., Visser, P. J., Philip, S., Frederik, B., & Tijms, B. M. (2022). Gray matter network properties show distinct associations with CSF p-tau 181 levels and amyloid status in individuals without dementia. *Aging Brain*, 2, 100054. <https://doi.org/10.1016/j.nbas.2022.100054>
- Montembeault, M., Rouleau, I., Provost, J.-S., & Brambati, S. M. (2015). Altered Gray Matter Structural Covariance Networks in Early Stages of Alzheimer's Disease. *Cerebral Cortex*, 26(6), 2650–2662. <https://doi.org/10.1093/cercor/bhv105>
- Márquez, F., & Yassa, M. A. (2019). Neuroimaging biomarkers for Alzheimer's Disease. *Molecular Neurodegeneration*, 14(1). <https://doi.org/10.1186/s13024-019-0325-5>
- Neu, S. C., Pa, J., Kukull, W., Beekly, D., Kuzma, A., Gangadharan, P., Wang, L.-S., Romero, K., Arneric, S. P., Redolfi, A., Orlandi, D., Frisoni, G. B., Au, R., Devine, S., Auerbach, S., Espinosa, A., Boda, M., Ruiz, A., Johnson, S. C., & Kosciak, R. (2017). Apolipoprotein E Genotype and Sex Risk Factors for Alzheimer Disease. *JAMA Neurology*, 74(10), 1178. <https://doi.org/10.1001/jamaneurol.2017.2188>
- Phillips, D. J., McGlaughlin, A., Ruth, D. M., Jager, L., & Soldan, A. (2015). Graph theoretic analysis of structural connectivity across the spectrum of Alzheimer's disease: The

importance of graph creation methods. *NeuroImage: Clinical*, 7, 377–390.

<https://doi.org/10.1016/j.nicl.2015.01.007>

Pelkmans, W., Ossenkoppele, R., Dicks, E., Strandberg, O., Frederik Barkhof, Pereira, J. B., & Hansson, O. (2021). Tau-related grey matter network breakdown across the Alzheimer's disease continuum. *Alzheimer's Research & Therapy*, 13(1).

<https://doi.org/10.1186/s13195-021-00876-7> (a)

Pelkmans, W., Legdeur, N., Ten Kate, M., Barkhof, F., Yaqub, M. M., Holstege, H., van Berckel, B. N. M., Scheltens, P., van der Flier, W. M., Visser, P. J., & Tijms, B. M. (2021). Amyloid- β , cortical thickness, and subsequent cognitive decline in cognitively normal oldest-old. *Annals of Clinical and Translational Neurology*, 8(2), 348–358.

<https://doi.org/10.1002/acn3.51273> (b)

Pelkmans, W., Vromen, E. M., Dicks, E., Scheltens, P., Teunissen, C. E., Barkhof, F., van der Flier, W. M., & Tijms, B. M. (2022). Grey matter network markers identify individuals with prodromal Alzheimer's disease who will show rapid clinical decline. *Brain Communications*, 4(2). <https://doi.org/10.1093/braincomms/fcac026>

Raffaele Cacciaglia, José Luís Molinuevo, Carles Falcón, Arenaza-Urquijo, E. M., Sánchez-Benavides, G., Brugulat-Serrat, A., Kaj Blennow, Zetterberg, H., Juan Domingo Gispert, Cañas, A., Carme Deulofeu, Dominguez, R., Fauria, K., Félez-Sánchez, M., de, G., Oriol Grau-Rivera, Hernández, L., Huesa, G., Huguet, J., & Marne, P. (2020). APOE- ϵ 4 Shapes the Cerebral Organization in Cognitively Intact Individuals as Reflected by Structural Gray Matter Networks. *Cerebral Cortex*, 30(7), 4110–4120.

<https://doi.org/10.1093/cercor/bhaa034>

Régy, M., Dugravot, A., Sabia, S., Fayosse, A., Mangin, J.-F., Chupin, M., Fischer, C., Bouteloup, V., Dufouil, C., Chêne, G., Paquet, C., Hanseeuw, B., Singh-Manoux, A., & Dumurgier, J. (2022). Association of APOE ϵ 4 with cerebral gray matter volumes in non-demented older adults: The MEMENTO cohort study. *NeuroImage*, 250, 118966.

<https://doi.org/10.1016/j.neuroimage.2022.118966>

Skup, M., Zhu, H., Wang, Y., Giovanello, K. S., Lin, J., Shen, D., Shi, F., Gao, W., Lin, W., Fan, Y., & Zhang, H. (2011). Sex differences in grey matter atrophy patterns among

AD and aMCI patients: Results from ADNI. *NeuroImage*, 56(3), 890–906.

<https://doi.org/10.1016/j.neuroimage.2011.02.060>

Sperling, R. A., Aisen, P. S., Beckett, L. A., Bennett, D. A., Craft, S., Fagan, A. M., Iwatsubo, T., Jack, C. R., Kaye, J., Montine, T. J., Park, D. C., Reiman, E. M., Rowe, C. C., Siemers, E., Stern, Y., Yaffe, K., Carrillo, M. C., Thies, B., Morrison-Bogorad, M., & Wagster, M. V. (2011). Toward defining the preclinical stages of Alzheimer's disease: Recommendations from the National Institute on Aging-Alzheimer's Association workgroups on diagnostic guidelines for Alzheimer's disease.

Alzheimer's & Dementia, 7(3), 280–292. <https://doi.org/10.1016/j.jalz.2011.03.003>

Tijms, B. M., Series, P., Willshaw, D. J., & Lawrie, S. M. (2011). Similarity-Based Extraction of Individual Networks from Gray Matter MRI Scans. *Cerebral Cortex*, 22(7), 1530–1541. <https://doi.org/10.1093/cercor/bhr221>

Tijms, B. M., Möller, C., Vrenken, H., Wink, A. M., de Haan, W., van der Flier, W. M., Stam, C. J., Scheltens, P., & Barkhof, F. (2013). Single-Subject Grey Matter Graphs in Alzheimer's Disease. *PLoS ONE*, 8(3).

<https://doi.org/10.1371/journal.pone.0058921> (a)

Tijms, B. M., Wink, A. M., de Haan, W., van der Flier, W. M., Stam, C. J., Scheltens, P., & Barkhof, F. (2013). Alzheimer's disease: connecting findings from graph theoretical studies of brain networks. *Neurobiology of Aging*, 34(8), 2023–2036.

<https://doi.org/10.1016/j.neurobiolaging.2013.02.020> (b)

Tijms, B. M., Mara ten Kate, Gouw, A. A., Borta, A., Verfaillie, S., Teunissen, C. E., Scheltens, P., Frederik Barkhof, & van. (2018). Gray matter networks and clinical progression in subjects with predementia Alzheimer's disease. *Neurobiology of Aging*, 61, 75–81. <https://doi.org/10.1016/j.neurobiolaging.2017.09.011>

ten Kate, M., Visser, P. J., Bakardjian, H., Barkhof, F., Sikkens, S. A. M., van der Flier, W. M., Scheltens, P., Hampel, H., Habert, M.-O., Dubois, B., & Tijms, B. M. (2018). Gray Matter Network Disruptions and Regional Amyloid Beta in Cognitively Normal Adults. *Frontiers in Aging Neuroscience*, 10.

<https://doi.org/10.3389/fnagi.2018.00067> (a)

ten Kate, M., Ingala, S., Schwarz, A. J., Fox, N. C., Chételat, G., van Berckel, B. N. M., Ewers, M., Foley, C., Gispert, J. D., Hill, D., Irizarry, M. C., Lammertsma, A. A., Molinuevo, J. L., Ritchie, C., Scheltens, P., Schmidt, M. E., Visser, P. J., Waldman, A., Wardlaw, J., & Haller, S. (2018). Secondary prevention of Alzheimer's dementia: neuroimaging contributions. *Alzheimer's Research & Therapy*, *10*(1).

<https://doi.org/10.1186/s13195-018-0438-z> (b)

Voevodskaya, O., Pereira, J. B., Volpe, G., Lindberg, O., Stomrud, E., van Westen, D., Westman, E., & Hansson, O. (2018). Altered structural network organization in cognitively normal individuals with amyloid pathology. *Neurobiology of Aging*, *64*, 15–24. <https://doi.org/10.1016/j.neurobiolaging.2017.11.014>

Vermunt, L., Dicks, E., Wang, G., Aylin Dincer, Flores, S., Keefe, S. J., Berman, S. B., Cash, D. M., Chhatwal, J. P., Cruchaga, C., Fox, N. C., Bernardino Ghetti, Graff-Radford, N. R., Hassenstab, J., Karch, C. M., Laske, C., Levin, J., Masters, C. L., McDade, E., & Mori, H. (2020). Single-subject grey matter network trajectories over the disease course of autosomal dominant Alzheimer's disease. *Brain Communications*, *2*(2).

<https://doi.org/10.1093/braincomms/fcaa102>

van Oostveen, W. M., & de Lange, E. C. M. (2021). Imaging Techniques in Alzheimer's Disease: A Review of Applications in Early Diagnosis and Longitudinal Monitoring. *International Journal of Molecular Sciences*, *22*(4), 2110.

<https://doi.org/10.3390/ijms22042110>

Yu, M., Sporns, O., & Saykin, A. J. (2021). The human connectome in Alzheimer disease — relationship to biomarkers and genetics. *Nature Reviews Neurology*, *17*(9), 545–563.

<https://doi.org/10.1038/s41582-021-00529-1>